Dark Matter and QCD-Charged Mediators in the Quasi-Degenerate Regime

Patrick Stengel

Stockholm University

February 22, 2018

1707.02460 with Andrew Davidson, Chris Kelso, Jason Kumar and Pearl Sandick

Squark mass limits from jets + MET searches

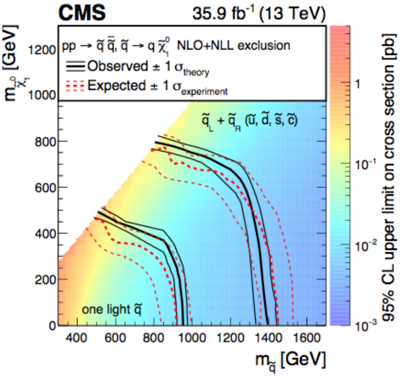

Figure: Simplified models only considering production of light flavor squark pairs, see *CMS 1704.07781*

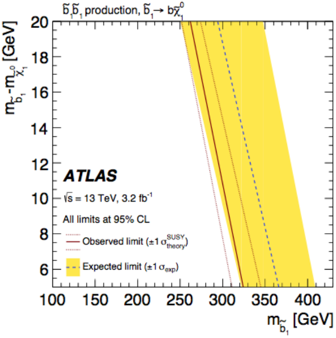

Figure: Use ISR to boost MET and help identify signal events, *ATLAS 1604.07773*

Resurrect "bulk" region by relaxing MFV, allowing light $\tilde{f}$

Light flavor squark co-annihilation

- pure $\widetilde{B}$ need sfermions with L-R mixing, nondegenerate masses for s-wave annihilation
- LHC less sensitive for $m_\chi \simeq m_{\tilde{q}} \gtrsim \mathcal{O}(400\,\mathrm{GeV})$
- need $\tilde{q}^*\tilde{q} \to gg$, $\chi\tilde{q} \to gq$

Scattering through squark exchange

- enhanced scattering cross section for $m_\chi \simeq m_{\tilde{q}}$
- need small mixing angle for consistency with SI limits
- dim-8/spin-dependent operators can dominate

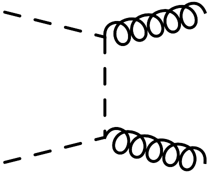

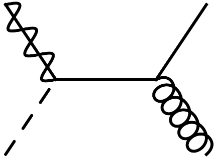

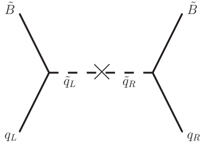

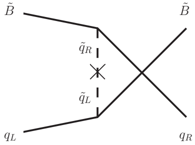

"Simplified" model with singlet DM, squark mediator(s)

$$\mathcal{L}_{int} = \sum_{q=u,d,s} \lambda_{Lq}(\bar{\chi} P_L q)\tilde{q}_L^* + \lambda_{Rq}(\bar{\chi} P_R q)\tilde{q}_R^* + h.c.$$

$$\tilde{q}_L = \tilde{q}_1 \cos\alpha + \tilde{q}_2 \sin\alpha$$

$$\tilde{q}_R = -\tilde{q}_1 \sin\alpha + \tilde{q}_2 \cos\alpha$$

Gauge invariance requires squark couplings to SM gauge bosons

$$\langle \sigma v(\tilde{q}^* \tilde{q} \to gg) \rangle = \frac{7 g_s^4 N_{\tilde{q}}}{432 \pi m_{\tilde{q}}^2} \left[N_{\tilde{q}} + \frac{\exp\left(\Delta m / T\right)}{3\left(1 + \Delta m / m_\chi\right)^{3/2}} \right]^{-2}$$

- For small $\Delta m = m_{\tilde{q}} - m_\chi$, QCD processes dominate annihilation
- Temperature at freeze out $T \simeq m_\chi/25$ for correct relic density
- Sum over $N_{\tilde{q}}$ mass degenerate light flavor squarks species

Co-annihilation processes needed to deplete relic desity

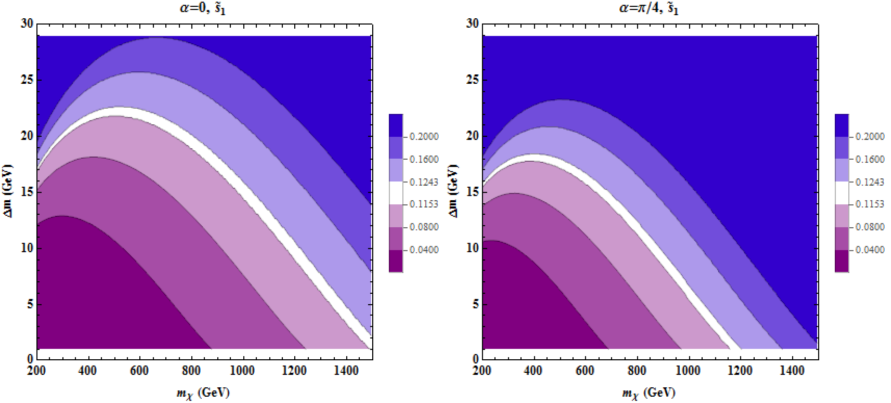

Figure: Relic density contours for benchmarks with a light d/s-type squark.

Adding squarks can raise or lower *effective* $\langle \sigma v \rangle$

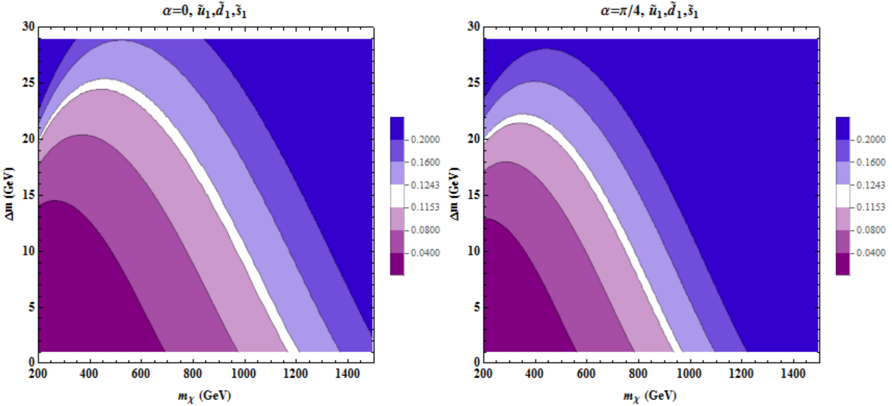

Figure: Relic density contours for benchmarks with light u-, d- and s-type squarks.

Relevant operators for squark exchange with $m_{\tilde{q}_1} \ll m_{\tilde{q}_2}$

$$\mathcal{O}_{q1} = \alpha_{q1}(\bar{\chi}\gamma^{\mu}\gamma^{5}\chi)(\bar{q}\gamma_{\mu}q)$$
$$\mathcal{O}_{q2} = \alpha_{q2}(\bar{\chi}\gamma^{\mu}\gamma^{5}\chi)(\bar{q}\gamma_{\mu}\gamma^{5}q)$$
$$\mathcal{O}_{q3} = \alpha_{q3}(\bar{\chi}\chi)(\bar{q}q)$$
$$\mathcal{O}_{qT2} = \alpha_{qT2}(\imath\bar{\chi}\gamma_{\mu}\partial_{\nu}\chi)\mathcal{O}_{q}^{(2)\mu\nu}$$

Scattering enhanced $m_{\chi} \simeq m_{\tilde{q}_1}$

- $\mathcal{O}_{q1^*,3,T2}$ spin independent
- $\mathcal{O}_{q2}$ spin dependent
- $\mathcal{O}_{q2,3,T2}$ velocity independent

$$\alpha_{q1,2} = \mp\left[\frac{|\lambda_L^2|}{8}\left(\frac{\cos^2\alpha}{m_{\tilde{q}_1}^2 - m_{\chi}^2}\right) + \frac{|\lambda_R^2|}{8}\left(\frac{\sin^2\alpha}{m_{\tilde{q}_1}^2 - m_{\chi}^2}\right)\right]$$
$$\alpha_{q3} = \frac{Re(\lambda_L\lambda_R^*)}{4}(\cos\alpha\sin\alpha)\left[\frac{1}{m_{\tilde{q}_1}^2 - m_{\chi}^2}\right]$$
$$\alpha_{qT2} = \frac{|\lambda_L^2|}{4}\left(\frac{\cos^2\alpha}{(m_{\tilde{q}_1}^2 - m_{\chi}^2)^2}\right) + \frac{|\lambda_R^2|}{4}\left(\frac{\sin^2\alpha}{(m_{\tilde{q}_1}^2 - m_{\chi}^2)^2}\right)$$

$\mathcal{O}_{q3}$ ($\mathcal{O}_{qT2}$) dominates in Xenon at large (small) mixing

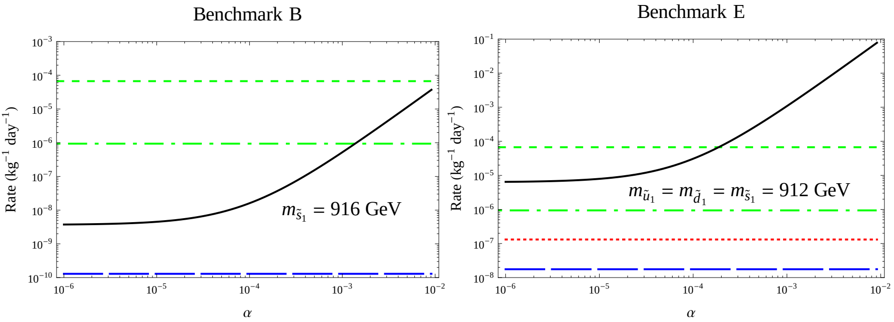

Figure: Event rate in Xenon-based detector as a function of α for $\mathcal{O}_{q1}$, $\mathcal{O}_{q2}$, $\mathcal{O}_{q3} + \mathcal{O}_{qT2}$, $m_\chi = 900\,\mathrm{GeV}$. Also show limits from XENON1T (dashed) and projections from LZ-7 (dash-dotted).

Projected sensitivity of direct detection at LZ-7

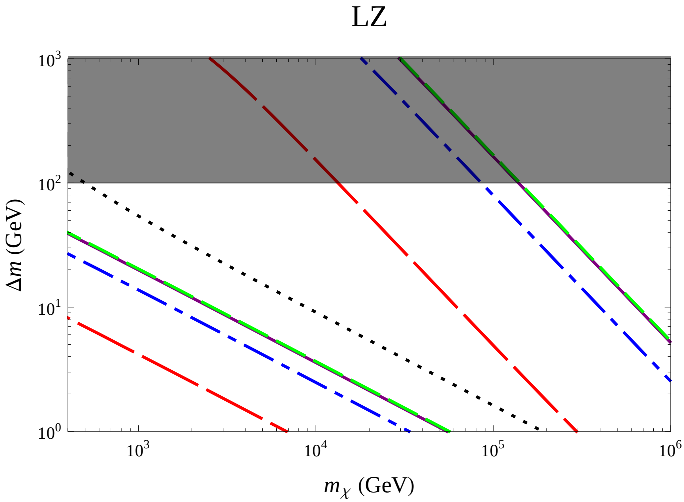

Figure: Projected LZ-7 sensitivity for benchmarks $\tilde{u}_1$, $\tilde{s}_1$, $\tilde{u}_1 \tilde{d}_1 \tilde{s}_1$, $\tilde{u}_1 \tilde{u}_2$.

Constraints applied to new MSSM paradigm

Light squark co-annihilation

- need $\tilde{q}\chi$ and $\tilde{q}\tilde{q}$ inital states to deplete relic density
- small mixing angle requires more general treatment of direct detection
- dim-8 or SD operators can dominate scattering at small α
- can probe squark masses higher than accessible at LHC

Slepton mediators

- for more "Incredible Bulk", see 1406.4903
- can look for compressed sleptons at LHC, **1706.05339**
- can probe full parameter space at ILC, **coming soon**
- direct (1608.00642), indirect (1605.03224) detection

Thank you!

Figure: See **1411.2634**

LSP is a natural WIMP candidate in the MSSM

R-parity suppresses proton decay

- $R = (-1)^{3B+L+2s}$
- Provides stable WIMP candidate

Neutralino in MSSM

- Mixture of neutral gauginos and higgsinos
- SM interactions depend on specific model
- mSUGRA tightly constrained

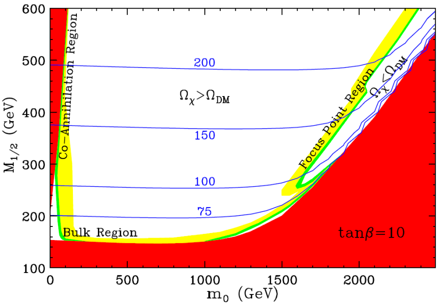

Figure: Cosmologically preferred mSUGRA regions are in green with $A_0 = 0$ and $\mu > 0$. Blue contours denote neutralino masses, see *Feng 1003.0904*.

Typical mSUGRA/CMSSM scenario with $\widetilde{B}$-$\widetilde{H}$ admixture

Relic density with $\bar{\chi}\chi \to WW, ff$

- Assuming gaugino mass unification (at least $M_1 \lesssim M_2$), yields neutralino with small $\widetilde{W}$
- Minimal flavor violation eliminates sfermion mixing
- Need $\mu/m_\chi \sim \mathcal{O}(1)$ for s-wave

see e.g. Feng, Sanford 1009.3934

SI scattering with Higgs exchange

- Scalar mediated interactions are velocity independent
- Minimal flavor violation guarantees coupling $\sim m_q$
- LHC data and $m_h \simeq 125\,\mathrm{GeV}$ push unified $m_{\tilde{f}} \gtrsim \mathcal{O}(\mathrm{TeV})$

see e.g. Baer et. al. 1112.3017

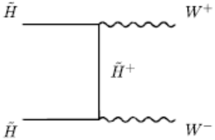

(a)Chargino-mediated Annihilation to W^+W^-

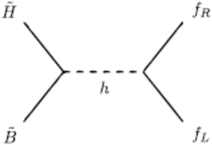

(c)Higgs-mediated Annihilation to Fermions

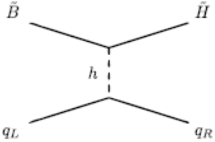

(a)Higgs-mediated Scattering

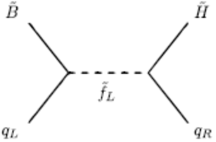

(b)Squark-mediated Scattering

Relic density for $\tilde{u}_1$

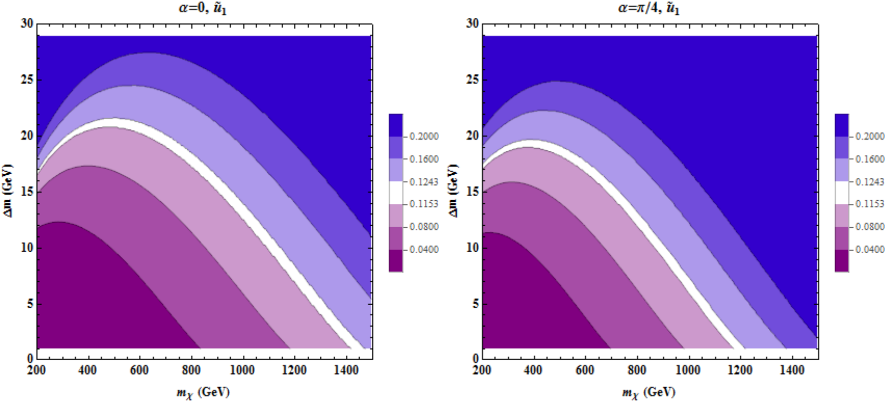

Figure: Relic density contours for benchmarks with light u–type squarks.

Relic density for $\tilde{u}_1\tilde{d}_1$

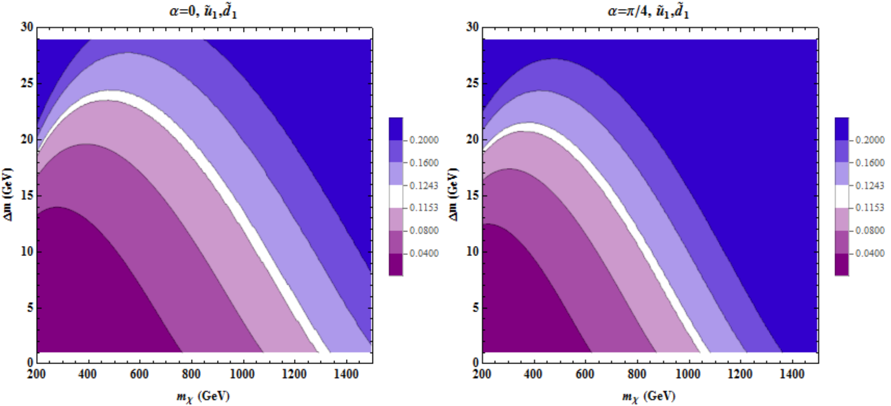

Figure: Relic density contours for benchmarks with light u- and d-type squarks.

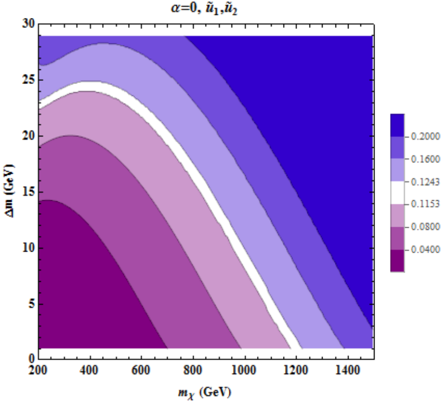

Figure: Relic density contours for benchmarks with two light u–type squarks.

$\tilde{u}_1$ and $\tilde{u}_1\tilde{u}_2$ in Xenon

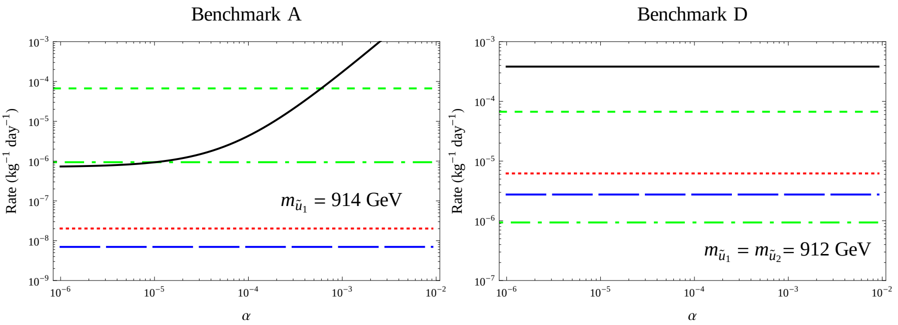

Figure: Event rate in Xenon-based detector as a function of α for $\mathcal{O}_{q1}$, $\mathcal{O}_{q2}$, $\mathcal{O}_{q3} + \mathcal{O}_{qT2}$, $m_\chi = 900\,\mathrm{GeV}$. Also show limits from XENON1T (dashed) and projections from LZ-7 (dash-dotted).

$\tilde{s}_1$ and $\tilde{u}_1\tilde{d}_1\tilde{s}_1$ in Fluorine

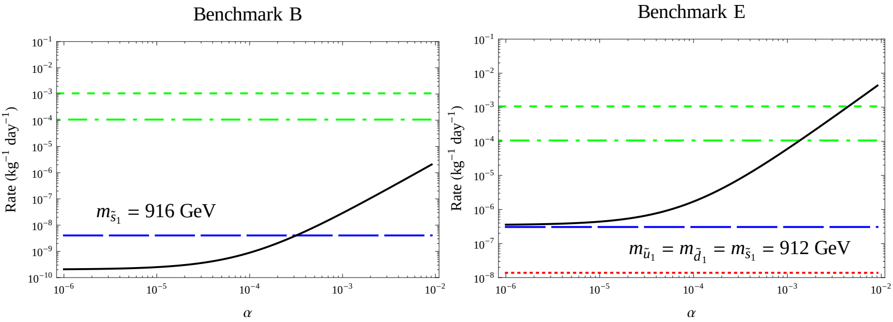

Figure: Event rate in Fluorine-based detector as a function of α for $\mathcal{O}_{q1}$, $\mathcal{O}_{q2}$, $\mathcal{O}_{q3} + \mathcal{O}_{qT2}$, $m_\chi = 900\,\mathrm{GeV}$. Also show limits from PICO-60L (dashed) and projections from PICO-250L (dash-dotted).

$\tilde{u}_1$ and $\tilde{u}_1\tilde{u}_2$ in Fluorine

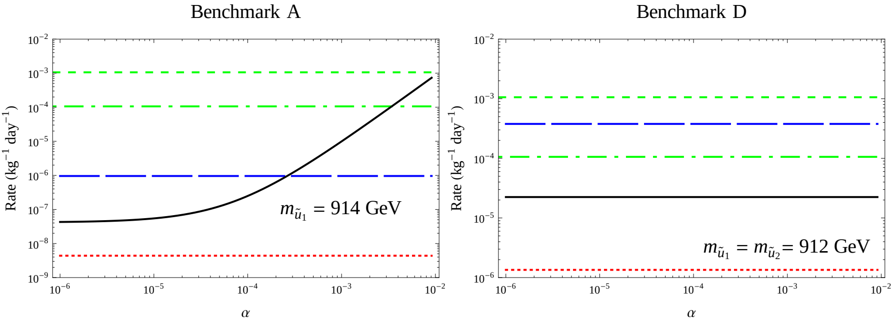

Figure: Event rate in Fluorine-based detector as a function of α for $\mathcal{O}_{q1}$, $\mathcal{O}_{q2}$, $\mathcal{O}_{q3} + \mathcal{O}_{qT2}$, $m_\chi = 900\,\mathrm{GeV}$. Also show limits from PICO-60L (dashed) and projections from PICO-250L (dash-dotted).

Current sensitivity of direct detection at XENON1T

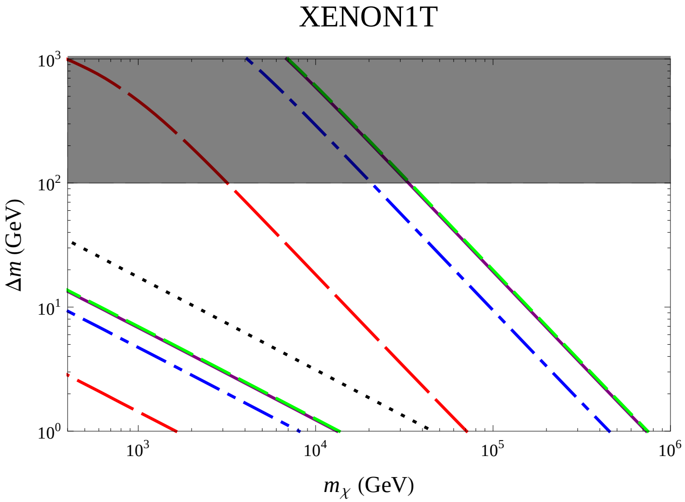

Figure: Current XENON1T sensitivity for benchmarks $\tilde{u}_1$, $\tilde{s}_1$, $\tilde{u}_1 \tilde{d}_1 \tilde{s}_1$, $\tilde{u}_1 \tilde{u}_2$.

Projected sensitivity of direct detection at PICO-250

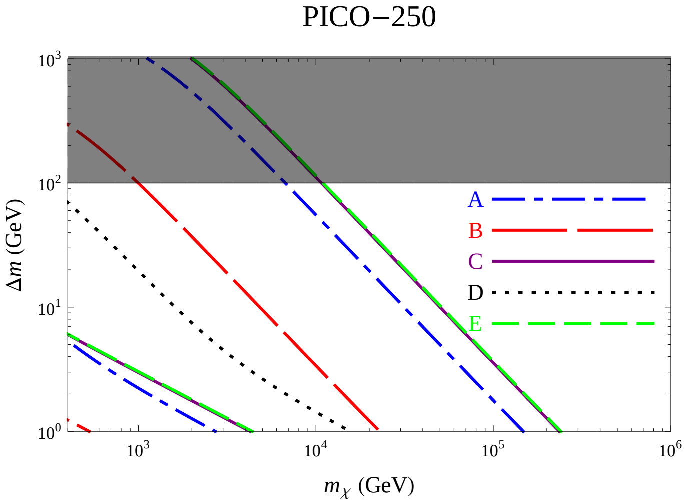

Figure: Projected PICO-250 sensitivity for benchmarks $\tilde{u}_1$, $\tilde{s}_1$, $\tilde{u}_1 \tilde{d}_1 \tilde{s}_1$, $\tilde{u}_1 \tilde{u}_2$.

Current sensitivity of direct detection at PICO-60

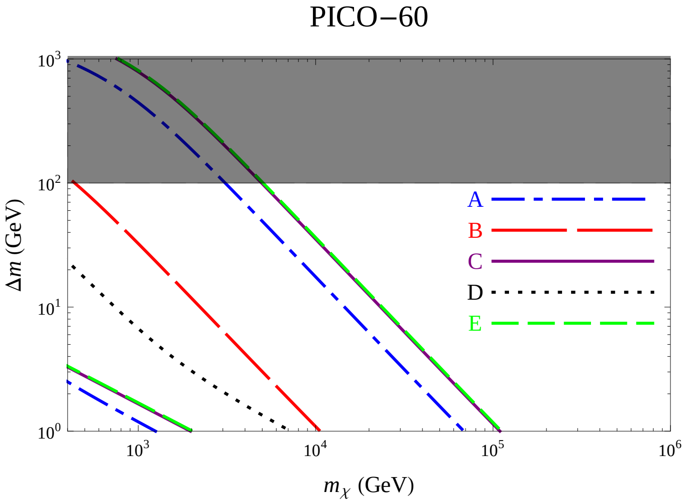

Figure: Current PICO-60 sensitivity for benchmarks $\tilde{u}_1$, $\tilde{s}_1$, $\tilde{u}_1 \tilde{d}_1 \tilde{s}_1$, $\tilde{u}_1 \tilde{u}_2$.

Can also satisfy relic density with L-R slepton mixing

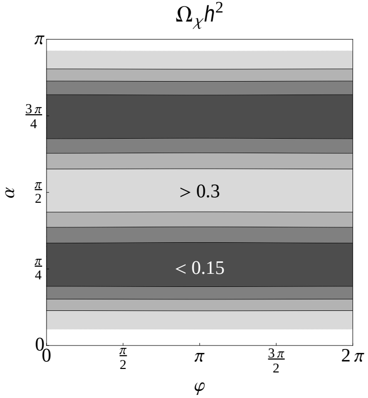

Figure: Bino relic abundance assuming smuon mixing with $m_\chi = 100\,\mathrm{GeV}$, $m_{\tilde{\mu}_1} = 120\,\mathrm{GeV}$ and $m_{\tilde{\mu}_2} = 300\,\mathrm{GeV}$.

$$\begin{aligned}
\mathcal{L}_{int} &= \lambda_L \tilde{\ell}_L \bar{\chi} P_L \ell + \lambda_R \tilde{\ell}_R \bar{\chi} P_R \ell \\
&\quad + \lambda_L^* \tilde{\ell}_L^* \bar{\chi} P_L l + \lambda_R^* \tilde{\ell}_R^* \bar{\chi} P_R \ell \\
\lambda_L &= \sqrt{2} g Y_L e^{\imath\phi/2} \\
\lambda_R &= \sqrt{2} g Y_R e^{-\imath\phi/2} \\
\begin{bmatrix} \tilde{\ell}_1 \\ \tilde{\ell}_2 \end{bmatrix} &= \begin{bmatrix} \cos\alpha & -\sin\alpha \\ \sin\alpha & \cos\alpha \end{bmatrix} \begin{bmatrix} \tilde{\ell}_L \\ \tilde{\ell}_R \end{bmatrix}
\end{aligned}$$

L-R mixing angle α, CP-violating phase ϕ

Dipole moments constrain mixing

Rule out $\tilde{e}$, constrain $\tilde{\mu}$, allow $\tilde{\tau}$

Can use ISR to boost MET and help S-B discrimination

$\tilde{\mu}_L$ with $30\,\mathrm{GeV} < \Delta m < 60\,\mathrm{GeV}$

- Can generally satisfy relic density with bino DM
- Do not need monojet for $\Delta m \gtrsim 70\,\mathrm{GeV}$
- Look for OSSF muons, one hard non-b jet and MET

Basic cuts reduce SM background

- $t\bar{t}$ needs one missed jet, both mistagged
- $Z \to \tau\bar{\tau} \to \ell^+\ell^- + 4\nu$ reduced by $M_{\tau\tau} > 125\,\mathrm{GeV}$

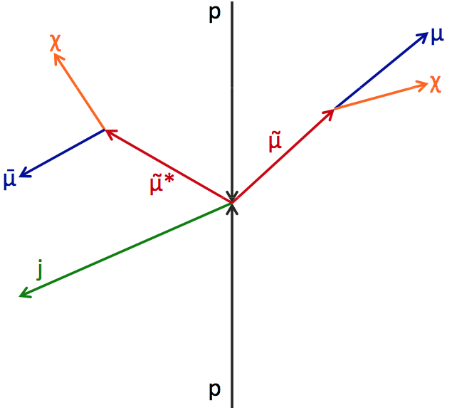

Angular variables can help reduce remaining backgrounds

Decay products collimated for parents produced above threshold

- $ZZ \to \ell^+\ell^-\nu\bar{\nu}$ leptons collimated, anti-collimated $\not{E}_T$
- $W^+W^- \to \ell^+\nu\ell^-\bar{\nu}$ leptons anti-collimated, collimated $\not{E}_T$

WW leptons, MET look like signal

- ISR boost smears collimation, $p_T(j)$ cut cannot be too high
- Less smearing for heavier parents, use rapidity to distinguish parent spin

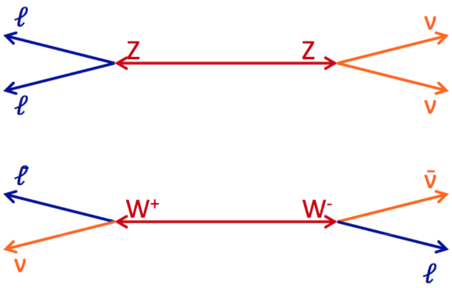

Figure: Credit J. Kumar

For $p_T(\ell) \ll p_T(j)$, signal MET balanced by $p_T(j)$

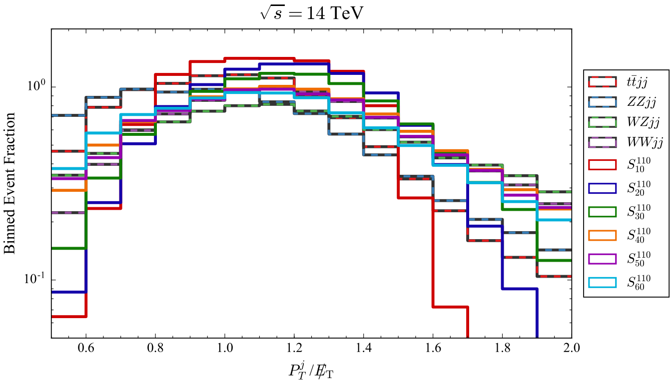

Figure: $1.0 < p_T(j)/\not{E}_T < 1.3$ cut for smaller mass differences

$ZZ \to \ell^+\ell^-\nu\bar{\nu}$ has leptons recoiling against MET

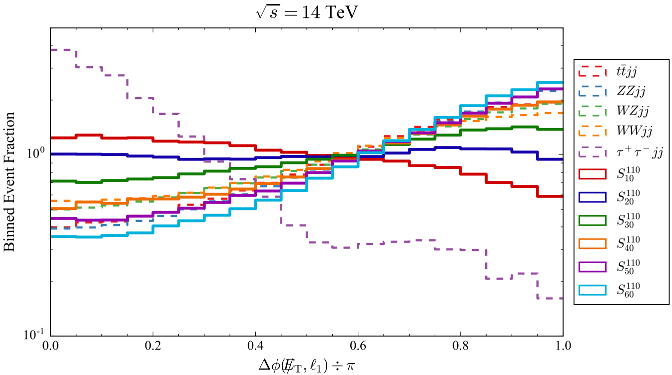

Figure: $\Delta\phi(\not{E}_T, \ell_1) < 0.6\pi$ helps for intermediate mass differences

$W^+W^- \to \ell^+\nu\ell^-\bar{\nu}$ has less anti-collimated leptons

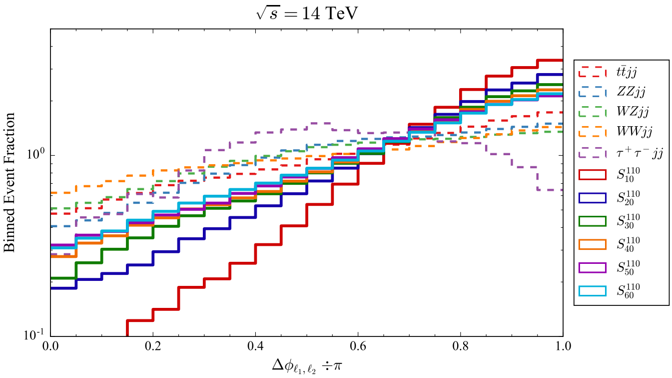

Figure: $\Delta\phi(\ell_1, \ell_2) > 0.5\pi$ suppresses background with lighter parents

$\cos\theta^*_{\ell_1,\ell_2} = \tanh(\Delta\eta_{\ell_1,\ell_2}/2)$ depends on parents' spin

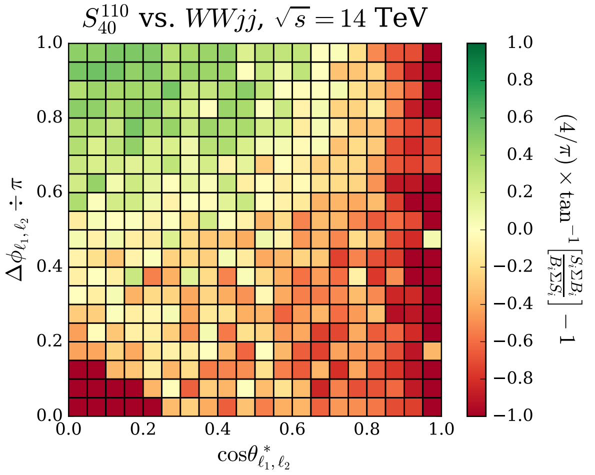

Figure: $\cos\theta^*_{\ell_1,\ell_2} < 0.5\pi$ suppresses background with spin-1 parents

Dipole moment contributions from L-R slepton mixing

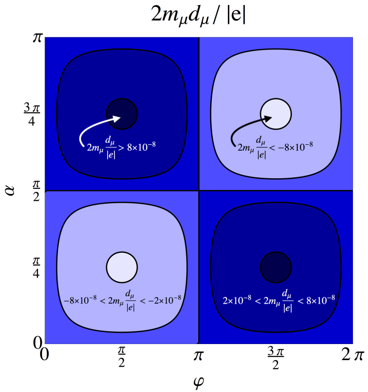

Figure: Muon electric dipole moment contribution assuming smuon mixing with $m_X = 100\,\mathrm{GeV}$, $m_{\tilde{\mu}_1} = 120\,\mathrm{GeV}$ and $m_{\tilde{\mu}_2} = 300\,\mathrm{GeV}$. All unconstrained.

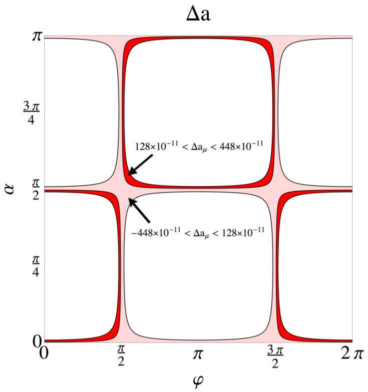

Figure: Muon magnetic dipole moment contribution either fully accounting for measured value (red) or only similar in magnitude (pink).

$M_{\tau\tau}$ supresses $Z \to \tau\bar{\tau}$

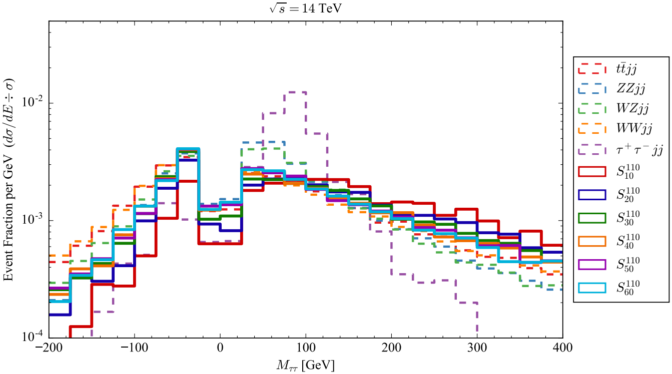

MET cut helps $t\bar{t}$ background

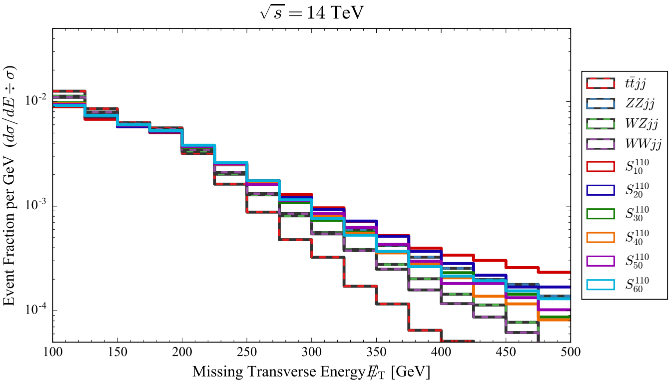

Window cut on $m_{\ell\ell}$ around m_Z

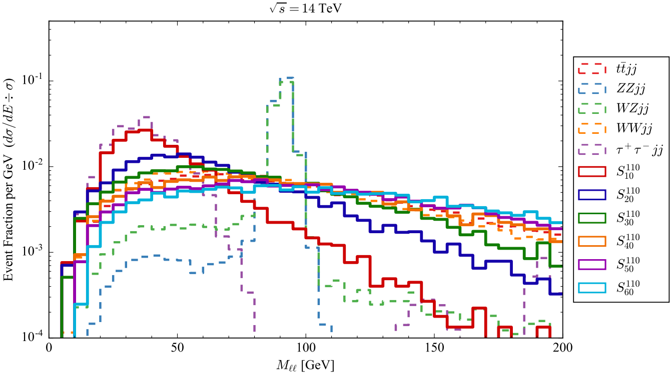

Leading lepton p_T

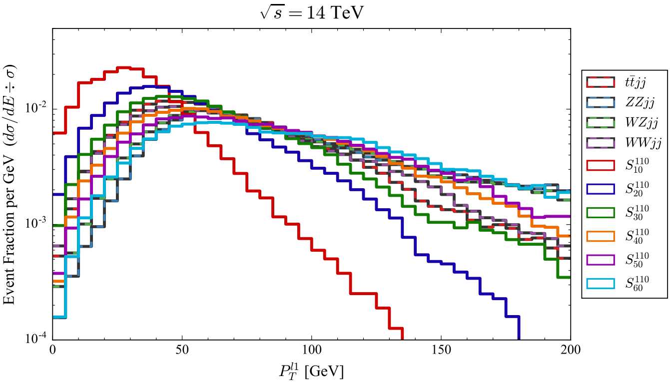

Subleading lepton p_T

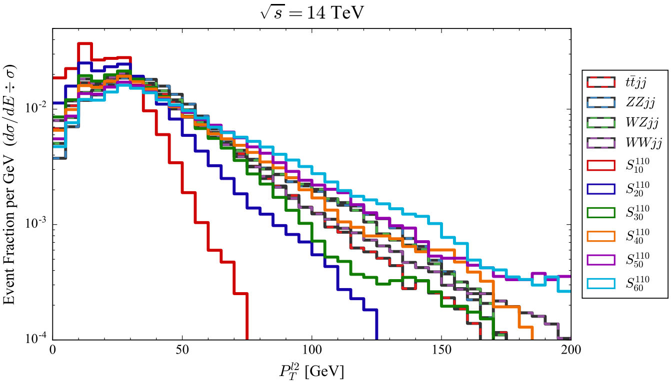

Primary and secondary cuts

Selection	$ZZjj$	$WZjj$	$WWjj$	S^{110}_{30}	S^{110}_{40}	S^{110}_{50}
Matched Production	1.3×10^4	4.2×10^4	9.5×10^4	1.9×10^2	1.9×10^2	1.9×10^2
τ-veto	1.2×10^4	4.0×10^4	8.9×10^4	1.9×10^2	1.9×10^2	1.9×10^2
OSSF muon	3.2×10^2	5.8×10^2	5.1×10^2	8.1×10^1	8.8×10^1	8.9×10^1
only 1J $P_T > 30$	9.4×10^1	1.5×10^2	1.1×10^2	1.6×10^1	1.7×10^1	1.7×10^1
Jet b-veto	8.0×10^1	1.4×10^2	1.1×10^2	1.6×10^1	1.7×10^1	1.7×10^1
$\not{E}_T > 100$ GeV	4.3×10^0	7.8×10^0	1.7×10^1	2.5×10^0	3.4×10^0	3.8×10^0
Jet $P_T > 100$ GeV	1.4×10^0	4.0×10^0	1.0×10^1	1.8×10^0	1.9×10^0	1.8×10^0
$m_{\ell\ell} \notin M_Z \pm 10$ GeV	1.0×10^{-1}	1.0×10^0	8.9×10^0	1.6×10^0	1.6×10^0	1.5×10^0
$m_{\tau\tau} > 175$ GeV	2.0×10^{-2}	3.3×10^{-1}	4.5×10^0	9.3×10^{-1}	9.3×10^{-1}	9.3×10^{-1}
$\not{E}_T > 175$ GeV	8.3×10^{-3}	9.9×10^{-2}	1.3×10^0	3.5×10^{-1}	3.1×10^{-1}	3.2×10^{-1}
Jet $P_T > 175$ GeV	6.6×10^{-3}	8.7×10^{-2}	1.2×10^0	3.3×10^{-1}	2.6×10^{-1}	2.6×10^{-1}

Tertiary cuts targeted at larger mass gaps

Selection	$ZZjj$	$WZjj$	$WWjj$	S^{110}_{30}	S^{110}_{40}	S^{110}_{50}
$M_{T2}^{WW} < 1$ GeV	3.9×10^{-3}	7.0×10^{-2}	8.6×10^{-1}	2.8×10^{-1}	2.1×10^{-1}	2.0×10^{-1}
$0.8 < P_T^j \div \not{E}_T < 1.8\}$	3.9×10^{-3}	5.6×10^{-2}	7.5×10^{-1}	2.7×10^{-1}	1.9×10^{-1}	1.7×10^{-1}
$\Delta\phi(\not{E}_T, \ell_1) \div \pi < 0.8$	3.9×10^{-3}	5.4×10^{-2}	7.2×10^{-1}	2.6×10^{-1}	1.9×10^{-1}	1.6×10^{-1}
$\Delta\phi(\ell_1, \ell_2) \div \pi > 0.5$	2.7×10^{-3}	3.1×10^{-2}	5.6×10^{-1}	2.0×10^{-1}	1.6×10^{-1}	1.2×10^{-1}
$P_T^{\ell 2} > 40$ GeV	0	1.1×10^{-2}	2.3×10^{-1}	9.4×10^{-2}	8.7×10^{-2}	8.4×10^{-2}
Events at $\mathcal{L} = 300\ \mathrm{fb}^{-1}$	0.0	3.4	68.5	28.2	26.1	25.2
$S \div B$	-	-	-	0.34	0.31	0.30
$S \div \sqrt{B}$	-	-	-	3.1	2.9	2.8
Poisson Significance	-	-	-	3.2	3.0	2.9

WIMP miracle predicts new physics at the weak scale

Stable, thermally produced particle will freeze out with relic abundance

$$\Omega_X \sim 1/\langle\sigma_A v\rangle$$

largely independent of DM mass, m_X

Assuming a weak coupling, dimensioanlly, the cross section

$$\langle\sigma_A v\rangle \sim \frac{g_{weak}^4}{m_X^2}(1 \text{ or } v^2)$$

$m_X \sim m_{weak}$ will yield the correct Ω_{DM} for s- or p-wave annihilation

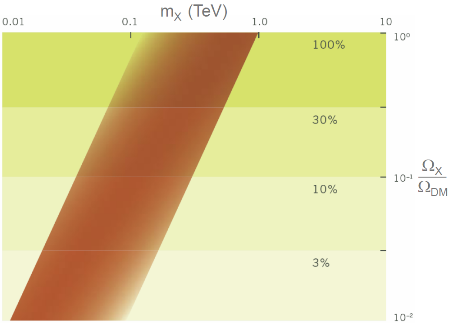

Figure: See Feng 1003.0904.

Weak scale DM motivated by new physics models

Stabilize gauge hierarchy problem → new weak scale particles

- Lightest new particle protected by discreet symmetry
- Provides WIMP candidate

Neutralino in MSSM

- Mixture of neutral gauginos and higgsinos
- SM interactions depend on specific model
- mSUGRA tightly constrained

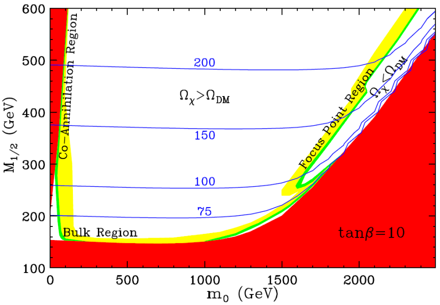

Figure: Cosmologically preferred mSUGRA regions are in green with $A_0 = 0$ and $\mu > 0$. Blue contours denote neutralino masses, see Feng 1003.0904.

MSSM parmeter space decouples into 3 sectors

- *Heavy sector*: Choose μ, heavy squark masses, and top trilinear couplings to obtain a SM Higgs. Decouple M_2, M_3 etc. to satisfy LHC.
- *Relic Density sector*: Choose slepton masses and mixings to achieve the dark matter relic abundance. Alternatively, the abundance may be achieved via coannihilations with squarks.
- *Direct Detection sector*: For a given bino mass, neutralino-nucleon elastic scattering cross sections are determined by the light squark masses and mixings.

PDF suppression of 2nd generation squark production

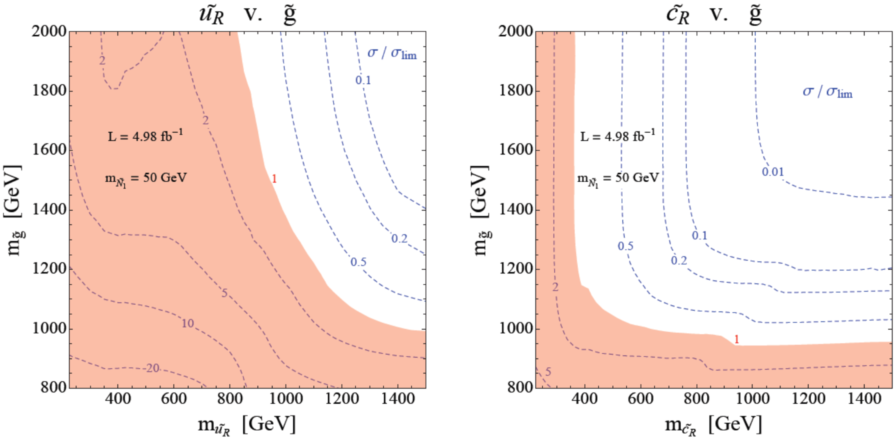

Figure: As $m_{\tilde{g}}$ falls, t-channel gluino exchange becomes important, see Mahbubani et. al. 1212.3328.

Scattering through scalar exchange in non-relativistic limit

$$
\begin{aligned}
\sigma_{SI}^{N} &= \frac{\mu_p^2}{32\pi(2J_X+1)} \sum_{spins} \left| \sum_q \frac{B_q^N}{m_X m_q} \mathcal{M}_{Xq\to Xq} \right|^2 \\
B_q^N &= \langle N|\bar{q}q|N\rangle = m_N\ f_q^N/m_q \\
B_u^p &= B_d^n = \tilde{\Sigma}_{\pi N} \left[1 + (1-y)\left(\frac{z-1}{z+1}\right)\right] \\
B_d^p &= B_u^n = \tilde{\Sigma}_{\pi N} \left[1 - (1-y)\left(\frac{z-1}{z+1}\right)\right] \\
B_s^p &= B_s^n = \tilde{\Sigma}_{\pi N}\, y,\ \ \Sigma_{\pi N} = (m_u + m_d)\tilde{\Sigma}_{\pi N}
\end{aligned}
$$

Largest uncertainty from strangeness content of nucleon $y = 1 - \sigma_0/\Sigma_{\pi N}$

$\Sigma_{\pi N} \sim 59\,\mathrm{MeV}$ can be determined from π-N scattering. $z \simeq 1.49$ and σ_0 can be fit from baryon octet mass differences in chiral pert. theory

Can also calculate σ_0 on the lattice and predict small $\Sigma_{\pi N}$

	$y \to 0$	$y = 0.06$	$y \to 1$
$B_u^p = B_d^n$	9.95 (7.59, 12.2)	9.85 (7.51, 12.1)	8.31 (6.34, 10.3)
$B_d^p = B_u^n$	6.67 (5.09, 8.38)	6.77 (5.17, 8.46)	8.31 (6.34, 10.3)
$B_s^p = B_s^n$	0	0.499 (0.380, 0.617)	8.31 (6.34, 10.3)

Table: Can end up with either small $\sigma_0 \lesssim \Sigma_{\pi N}$ or $\sigma_0 \sim \Sigma_{\pi N}$. We assume the central value for $\Sigma_{\pi N}$ of 59 MeV, with the numbers in parentheses indicating the 2σ range for $\Sigma_{\pi N}$ (45 MeV, 73 MeV), see Alarcon, Camalich, Oller 1110.3797.

$$B^N_{q=c,b,t} = \frac{2}{27}\frac{m_N}{m_q} f_g^N, \;\; f_g^N = 1 - \sum_{q=u,d,s} f_q^N$$

Quark loops could couple heavy flavor squarks to gluon content in nucleon

Recall, for squark mixing, we have $\mathcal{M}_{Xq \to Xq} \sim m_q$, so $q = c, b, t$ contributions to σ_{SI}^N will be suppressed by m_q^{-2} without MFV couplings.

Calculate cross section and check dipole moments

$$\sigma_{SI}^N = \frac{\mu_p^2}{4\pi}\left\{\sum_q g^2 Y_L Y_{Rq} \sin(2\phi_{\tilde{q}}) \left[\frac{1}{(m_{\tilde{q}_1}^2 - m_X^2)} - \frac{1}{(m_{\tilde{q}_2}^2 - m_X^2)}\right] B_q^N \lambda_q\right\}^2$$

where λ_q accounts for running from the weak scale. For $m_X \ll m_{\tilde{q}_1} \ll m_{\tilde{q}_2}$

$$\frac{\Delta a}{m_q} \sim \frac{m_X}{16\pi^2 m_{\tilde{q}_1}^2} g^2 Y_L Y_{Rq} \sin(2\phi_{\tilde{q}})$$

$$\sigma_{SI}^N \sim (1.1 \times 10^9 \ \mathrm{pb\,GeV}^2) \left(\sum_q \frac{\Delta a_q}{m_q} \frac{B_q^N}{0.5}\right)^2 \left(\frac{m_X}{50 \ \mathrm{GeV}}\right)^{-2}$$

Direct detection already rules out models with $\Delta a_q(\mathrm{GeV}/m_q) \gtrsim 10^{-9}$

No contribution to quark EDM and quark MDM limits are relatively weak

LEP constrains current quark moments by checking Γ_Z contributions and LHC constrains chromomagnetic moments; most stringent $\Delta a_q \lesssim 10^{-5}$

Assume $m_X = 50\ \mathrm{GeV}$, maximal mixing and minimal B_s^N

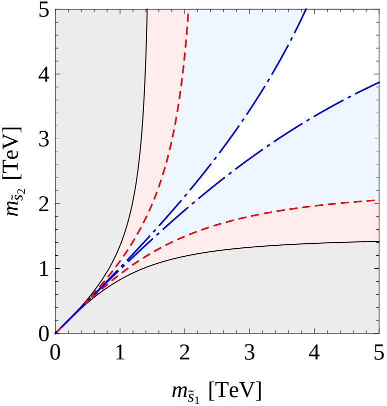

Figure: The grey region is ruled out by **LUX**, the red region could be ruled out by 300 days of LUX data and the blue region could be probed by LZ-7.

Direct detection with decoupled $m_{\tilde{s}_2}$ and minimal B_s^N

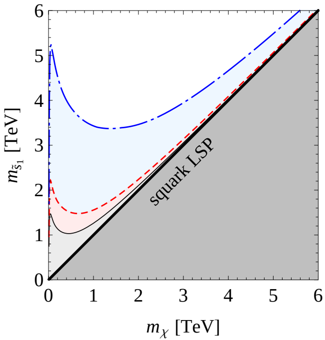

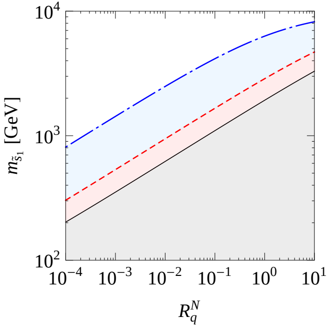

Figure: Sensitivity in the $(m_X, m_{\tilde{s}_1})$ plane assuming maximal mixing (left) and $(R_s^N, m_{\tilde{s}_1})$ plane with $R_q^N \equiv Y_{Rq}^2 \sin^2(2\phi_{\tilde{q}})(B_q^N)^2\lambda_q^2$ and $m_X = 50\ \mathrm{GeV}$ (right).

$$\sigma_{SI}^N \sim \frac{\mu_p^2 R_q^N}{(m_{\tilde{q}_1}^2 - m_X^2)^2}$$

- Enhanced sensitivity near $m_\chi \simeq m_{\tilde{q}_1}$
- Squark mass reach comperable to LHC

Uncertainty in SI scattering due to strangeness content

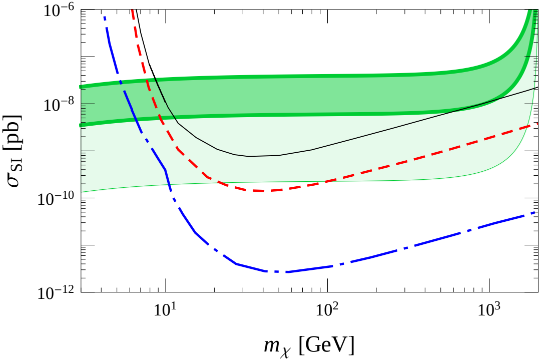

Figure: Sensitivity in the $(m_{\tilde{\chi}}, \sigma^N_{SI})$ plane with with $m_{\tilde{s}_1} = 2\ \mathrm{TeV}$ and maximal mixing. The dark green band indicates the predicted SI-scattering cross section for $\sigma_0 = 27\ \mathrm{MeV}$ and allowing the full 2σ range for $\Sigma_{\pi N}$ of 45 MeV to 73 MeV.